

The Phosphatases STS1 and STS2 Regulate Hematopoietic Stem and Progenitor Cell Fitness

Jing Zhang,^{1,2,3} Olesya Vakhrusheva,¹ Srinivasa Rao Bandi,¹ Özlem Demirel,^{1,2,3} Julhash U. Kazi,⁴ Ramona Gomes Fernandes,¹ Katja Jakobi,^{1,2,3} Astrid Eichler,¹ Lars Rönstrand,⁴ Michael A. Rieger,^{1,2,3} Nick Carpino,⁵ Hubert Serve,^{1,2,3} and Christian H. Brandts^{1,2,3,*}

¹Department of Medicine, Hematology/Oncology, Goethe University, 60590 Frankfurt, Germany

²German Cancer Consortium, 69120 Heidelberg, Germany

³German Cancer Research Center, 69120 Heidelberg, Germany

⁴Division of Translational Cancer Research and Lund Stem Cell Center, Lund University, Medicon Village, 22363 Lund, Sweden

⁵Department of Molecular Genetics and Microbiology, Stony Brook University, Stony Brook, NY 11794, USA

*Correspondence: brandts@em.uni-frankfurt.de

<http://dx.doi.org/10.1016/j.stemcr.2015.08.006>

This is an open access article under the CC BY-NC-ND license (<http://creativecommons.org/licenses/by-nc-nd/4.0/>).

SUMMARY

FLT3 and c-KIT are crucial regulators of hematopoietic stem and progenitor cells. We investigated the role of STS1 and STS2 on FLT3 and c-KIT phosphorylation, activity, and function in normal and stress-induced hematopoiesis. STS1/STS2-deficient mice show a profound expansion of multipotent progenitor and lymphoid primed multipotent progenitor cells with elevated colony-forming capacity. Although long-term hematopoietic stem cells are not increased in numbers, lack of STS1 and STS2 significantly promotes long-term repopulation activity, demonstrating a pivotal role of STS1/STS2 in regulating hematopoietic stem and progenitor cell fitness. Biochemical analysis identified STS1/STS2 as direct phosphatases of FLT3 and c-KIT. Loss of STS1/STS2 induces hyperphosphorylation of FLT3, enhances AKT signaling, and confers a strong proliferative advantage. Therefore, our study reveals that STS1 and STS2 may serve as novel pharmaceutical targets to improve hematopoietic recovery after bone marrow transplantation.

INTRODUCTION

Hematopoietic stem cells (HSCs) are capable of both self-renewal and production of mature blood lineages. Players in this balanced regulation include transcription factors, cell-cycle regulators, signaling molecules, surface receptors, and cytokines (Rossi et al., 2012). The type III receptor tyrosine kinases (RTKs), which include FMS-like tyrosine kinase-3 (FLT3), c-KIT (referred to hereafter as KIT), cFMS, and PDGFR play a key role in normal and malignant hematopoiesis. Importantly, FLT3 and KIT are highly expressed on hematopoietic stem and progenitor cells (HSPCs) (Adolfsson et al., 2005; Boyer et al., 2011; Buza-Vidas et al., 2009) as well as on the surface of leukemic blasts in most patients with acute myeloid leukemia (Sargin et al., 2007; Toffalini and Demoulin, 2010).

Extracellular binding of a specific ligand to its respective RTK induces dimerization and autophosphorylation on specific tyrosine residues, followed by activation of intracellular signaling cascades. The amplitude and duration of RTK signaling is tightly controlled by receptor ubiquitination, internalization, and degradation, resulting in signal termination (Verstraete and Savvides, 2012). In this context, E3 ligases mediate ubiquitination, thereby initiating internalization and endocytosis (Ryan et al., 2006; Toffalini and Demoulin, 2010; Verstraete and Savvides, 2012). Dephosphorylation of RTKs by phosphatases has been less studied so far and appears to be a transient and

fine-tuned negative regulation of RTK signaling (Dikic and Giordano, 2003; Sastry and Elferink, 2011).

We have reported previously that the E3 ligase CBL binds to autophosphorylated FLT3 and KIT and leads to FLT3 and KIT ubiquitination via its E3 ligase activity (Bandi et al., 2009; Sargin et al., 2007). It has been shown that FLT3 signaling is greatly amplified in FLT3⁺ multipotent progenitors (MPPs) in a genetic mouse model expressing a RING finger mutant of CBL, leading to a myeloid proliferative disease. This phenotype was reversible by treatment with the FLT3 kinase inhibitor AC220 (Rathinam et al., 2010; Taylor et al., 2012). Here we analyze the function of two known binding partners of CBL and evaluate their potential phosphatase activity toward FLT3 and KIT: STS1 and STS2 (suppressor of T cell receptor signaling 1 and 2, also known as TULA2 and TULA and UBASH3B and UBASH3A, respectively). STS1 and STS2 proteins share a 75% amino acid homology and are characterized by a ubiquitin binding domain (UBA), a SH3 domain, and a phosphoglycerate mutase-like domain (PGM) (Carpino et al., 2002, 2004). Both proteins bind CBL through their SH3 domain and regulate interactions between trafficking receptors and the ubiquitin sorting machinery in the endosome through their UBA domain (Kowanetz et al., 2004; Mikhailik et al., 2007; Raguz et al., 2007). STS1/STS2 have been shown to constitutively interact with CBL and inhibit CBL-mediated degradation of the epidermal growth factor (EGF) receptor (Feshchenko et al., 2004; Raguz et al., 2007). Importantly,

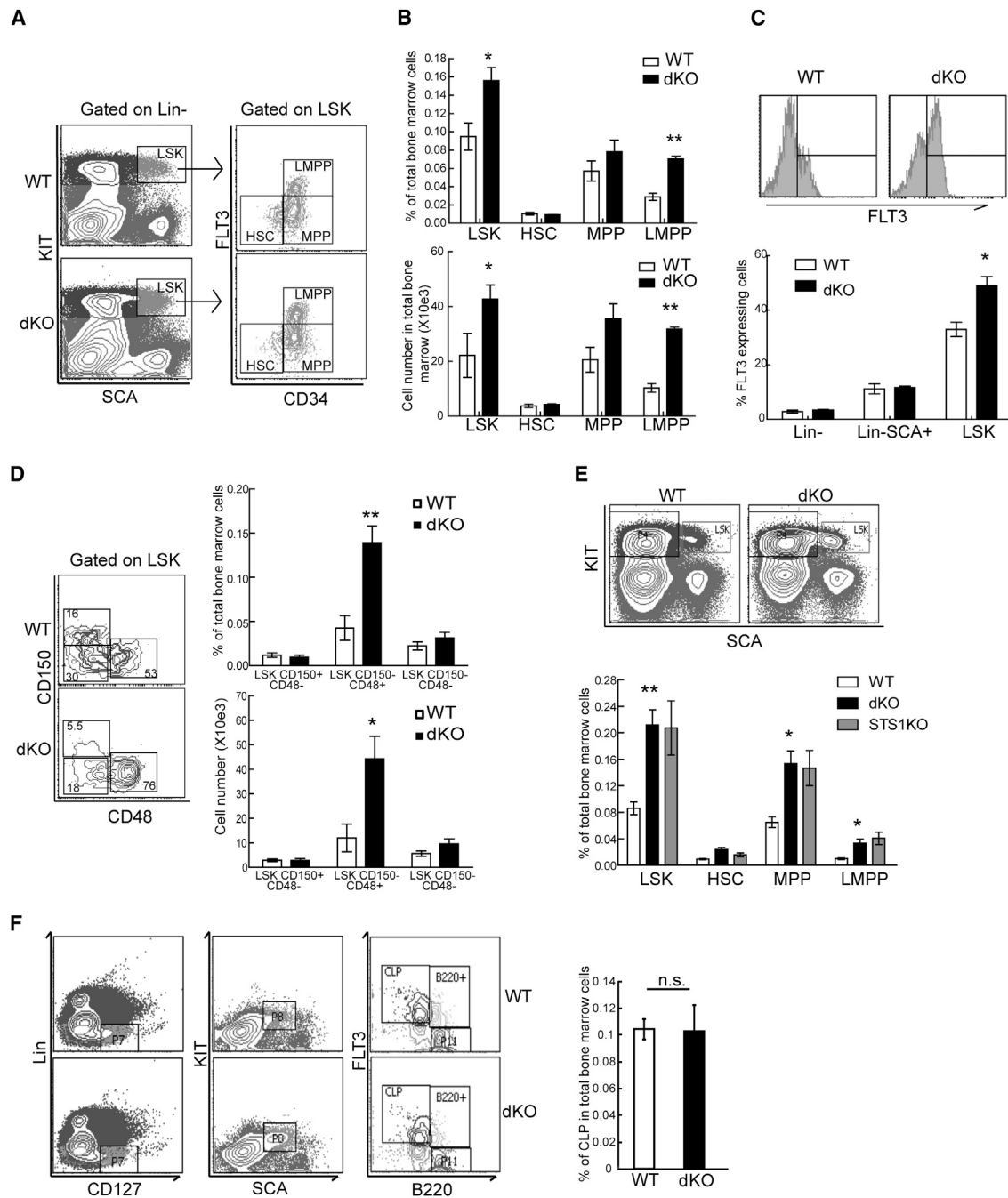


Figure 1. Loss of STS1/STS2 Leads to Expansion of MPP and LMPP Cell Populations

(A) Representative FACS staining plots showing LSK (Lin⁻SCA⁺KIT⁺) compartment distribution (left) and HSC (LSKFLT3⁻CD34⁻), MPP (LSKFLT3⁻CD34⁺), LMPP (LSKFLT3⁺CD34⁺) distribution (right) in 4-month-old mice.

(B) Quantification of LSK cell frequency (top) and absolute numbers in double tibias and femurs (bottom) in 4-month-old mice (n = 3).

(C) Representative FACS staining plots (top) and percentage of FLT3⁺ cells within lineage-negative (Lin⁻), Lin⁻SCA⁺, or LSK compartments

(bottom) in 4-month-old mice (n = 3).

(D) Representative FACS staining plots and quantification of CD150 and CD48 staining populations within the LSK compartment in 9-month-old mice (n = 5).

(legend continued on next page)



STS1 has been shown to be a tyrosine phosphatase for the EGF and PDGF receptors, with the PGM domain encoding the phosphatase activity (Hoeller et al., 2006; Mikhailik et al., 2007). Interestingly, the phosphatase activity of STS2 is much weaker, although the PGM domains of STS1 and STS2 are highly homologous (Carpino et al., 2009; Chen et al., 2009a, 2009b). Single STS1 or STS2 knockout mice are viable, develop normally, and do not display any obvious abnormalities, and no differences were detected concerning bone marrow cellularity, B and T cell development, or proliferative capacity. Mice lacking both STS proteins are shown to be hyper-responsive to T cell receptor stimulation, resulting in an increase in both cytokine production and susceptibility to autoimmunity (Carpino et al., 2002, 2004).

The effect of STS1/STS2 on FLT3 and KIT and the functional consequences for hematopoiesis are unknown. By combining the genetic STS1/STS2 knockout mouse model with appropriate biochemical tools, we have analyzed the effect of STS1 and STS2 on HSPCs and FLT3/KIT-dependent signaling.

RESULTS

Loss of STS1 and STS2 Leads to a Phenotypic Expansion of the MPP and Lymphoid-Primed MPP Cell Populations

Defined hematopoietic compartments were separated, by fluorescence-activated cell sorting (FACS), from the bone marrow (BM) of wild-type (WT) C57BL/6 mice and analyzed by real-time PCR, demonstrating that *Sts1* and *Sts2* mRNA was expressed in HSPCs (Figure S1A).

The hematopoietic compartments of STS1^{-/-} and STS2^{-/-} knockout (STS1KO and STS2KO) mice as well as of STS1^{-/-}/STS2^{-/-} double knockout (dKO) mice underwent detailed phenotypic characterization. However, FACS analysis revealed a remarkable relative and absolute increase in Lin⁻SCA⁺KIT⁺ (LSK) cells in the bone marrow of dKO mice (Figures 1A, 1B, and 1E). This difference was already significant in 4-month-old mice (Figure 1B) and enhanced further with age in 12- to 14-month-old mice (Figure 1E). Notably, the increased LSK population in dKO mice is attributable to MPPs (LSK FLT3⁻CD34⁺) and FLT3⁺MPP/lymphoid-primed MPPs (LMPPs) (LSK FLT3⁺CD34⁺) (Figures 1B and 1E), which are considered to be multipotent progenitor cells with limited or no self-renewal activity (Adolfsson et al., 2005; Yamamoto et al.,

2013). In contrast, we found no significant difference in the HSC (LSK FLT3⁻CD34⁻) compartment (Figures 1B and 1E). This phenotype appears to be largely due to the loss of STS1 (Figure 1E) but not STS2 (Figures S1B–S1E). However, STS1 KO cells appear to have a more variable phenotype (i.e., larger error bars; Figure 1E) compared with dKO cells.

Importantly, although there was only a minor gain in the mean surface expression intensity (data not shown), the relative frequency of FLT3⁺ bone marrow cells was increased greatly in dKO mice within LSK cells compared with the WT (Figure 1C) and, to a lesser degree, KIT⁺ as well (data not shown).

As we postulated that loss of STS1/STS2 affects FLT3 surface expression, we sought for independent markers to support our findings by using the signaling lymphocyte activation module (SLAM) markers CD150 and CD48 (Kiel et al., 2005; Yilmaz et al., 2006). As shown in Figure 1D, left, we again observed a significant expansion of CD150⁻CD48⁺ population at the expense of the CD150⁺CD48⁻ cells within LSK population. However, because of the expansion of the LSK population, no differences in the absolute number or frequency of HSCs (LSK CD150⁺CD48⁻) were found in the bone marrow, whereas MPPs/LMPPs (LSK CD150⁻CD48^{-/+}) were increased greatly in dKO mice (Figure 1D, right).

There was no significant shift of myeloid progenitor (megakaryocyte-erythroid progenitor [MEP], common myeloid progenitor [CMP], and granulocyte-macrophage progenitor [GMP]) populations between WT and dKO mice (Figure S2A). Furthermore, although lymphoid progenitor populations were largely determined by FLT3 expression (Adolfsson et al., 2005; Karsunky et al., 2008; Mackarechtschian et al., 1995), the percentage of the common lymphoid progenitor (CLP, Lin⁻CD127⁺KIT^{int}SCA^{int}FLT3⁺B220⁻) cell population remained unchanged between genotypes (Figure 1F). However, as reported previously, dKO mice display an increased B cell and decreased T cell population in the spleen and peripheral blood (Figure S2B; Carpino et al., 2004), indicating a skewing within lymphoid cells.

Taken together, depletion of STS1 and STS2 leads to a phenotypic expansion of the MPP and LMPP populations.

Increased Colony-Forming Capacity of dKO Bone Marrow Cells

Given the phenotypic enrichment of LSK in dKO mice (Figure 1), we asked whether this leads to functional differences. In serial colony-forming assays, no differences were

(E) Representative FACS staining plots (top) and quantification of LSK, HSC, MPP, and LMPP cell frequency (bottom) in 14-month-old mice (n = 4).

(F) Representative FACS staining plots showing CLP (Lin⁻KIT^{int}SCA^{int}CD127⁺FLT3⁺B220⁻) compartment distribution (left) and quantification of CLP cell frequency (right) in 6-month-old mice (WT and dKO, n = 4; STS1KO, n = 3).

(B–F) Data represent mean ± SEM. *p < 0.05; **p < 0.01; n.s., not significant (Student's t test). See also Figures S1 and S2.



observed in the initial plating, whereas STS1/STS2-deficient total bone marrow cells generated significantly more colonies from the second replating onward (Figure 2A). Types of colonies did not differ between genotypes (Figure 2B). Furthermore, LSK cells from dKO mice not only gave rise to more colonies (Figure 2C), but, most importantly, these colonies displayed higher cell numbers (Figure 2D). Morphological classification of the colonies indicates a trend toward increased colony-forming unit-granulocyte/macrophages (CFU-GMs) and decreased CFU-megakaryocytes (CFU-Ms) (Figure 2E). This expansion of cell numbers was mostly attributed to the loss of STS1, albeit with higher variability compared with dKO (Figures 2C and 2D). Surface marker analysis of these cells revealed an accumulation of less differentiated cells (defined as MAC-1⁻ KIT⁺ CD48⁺ CD16/32⁻; Figure 2F) in dKO mice. No changes were found in the differentiation markers GR1, MAC-1, CD71, and CD19 (data not shown). These findings indicate that the absence of STS1 and STS2 does not significantly alter the terminal lineage differentiation but, rather, the expansion of more immature cells.

To confirm the *in vitro* data, we performed a CFU-S assay (colony-forming units in spleen) with WT and dKO bone marrow cells as donors. As shown in Figure 2G, we observed a significantly increased colony number in dKO donors, functionally confirming the phenotypically increased MPP/LMPP populations. Importantly, significantly decreased colony growth was demonstrated in AC220-treated mice. The colony numbers were decreased significantly in dKO donors and resulted in equal numbers as WT donors (Figure 2G).

Enhanced Long-Term Repopulation Capacity of STS1/STS2-Depleted HSCs

To investigate the long-term repopulation capacity of dKO HSCs, we performed a competitive transplantation experiment, as depicted schematically in Figure 3A. When total bone marrow cells were used as the donor source, hematopoietic repopulation was very similar in dKO and WT cells until week 8. Thereafter, hematopoiesis derived from dKO donor mice expanded faster than in WT donor cells (Figure 3B), which is most likely a reflection of the higher LSK cell content in dKO mice (Figures 1B and 1E). We then asked whether the phenotypically increased MPPs/LMPPs from dKO mice acquired long-term repopulation activity. Therefore, we transplanted the same numbers of LMPP cells (LSKCD150⁻CD48⁺) and found a significantly higher engraftment of cells lacking STS1/STS2 at early time points (4 weeks) but not at later time points (from 8 weeks onward; Figure 3C). Staining of the lineage marker showed a strikingly increased T cell population and decreased B cell population (Figure 3D; Figure S3A). These data demonstrate, on one hand, that LMPP cells from

dKO mice have enhanced short-term repopulation ability because of increased fitness and, on the other hand, that they exhibit no long-term repopulation capacity.

Next we transplanted sorted LSK cells (which phenotypically contain equal or less HSCs in dKO because of the expansion of MPPs/LMPPs) into WT recipient mice. In the primary recipients, no difference in the engraftment, expansion, or differentiation of donor cells was found in the peripheral blood (Figures 3E and 3F; Figure S3B). However, bone marrow analysis showed a trend toward a higher LSK and LSKCD34⁻ cell percentage in dKO cells (Figure 3G). Importantly, when the bone marrow cells from this transplantation were re-transplanted into secondary recipients, a significantly enhanced engraftment of STS1/STS2-depleted cells was observed (Figure 3H), with a shift from T to B cells in dKO mice after 8 weeks after the second transplantation (Figure 3I; Figure S3C). Consistently, LSK cells (both CD34⁺ and CD34⁻) from dKO mice were increased significantly, suggesting a tremendous functional growth advantage of dKO over WT cells (Figure 3J). Therefore, although no differences were found in primary recipients (Figures 3E and 3G), we observed a dramatically enhanced expansion of dKO donor cells in the spleens and bone marrow of secondary recipient mice (Figures 3K and 3L, respectively). These differences could, in principle, be explained by increased homing. We therefore studied the homing capacity of lineage-negative bone marrow cells in lethally irradiated recipients and found reduced homing of dKO bone marrow cells (Figure 3M). These data strongly argue against increased homing as the explanation for the significant expansion of dKO cells.

Taken together, the functional analyses demonstrate that, LMPPs lacking STS1/STS2 exhibit a short-lived repopulation advantage, whereas HSCs from dKO mice have a remarkably enhanced capacity for long-term repopulation after secondary transplantation. This indicates that loss of STS1/STS2 endows both multipotent progenitors as well as HSCs with increased cell fitness.

STS1 Dephosphorylates FLT3 and KIT

Given the phenotypic and functional changes identified in dKO, we aimed to investigate the molecular mechanism whereby STS1 and STS2 may affect MPP/LMPP expansion and HSC maintenance. As depicted in Figure 1C, FLT3⁺ cells are strongly enriched in the bone marrow of dKO mice. Since STS1 has been demonstrated to be a phosphatase of the EGF receptor, we asked whether FLT3 phosphorylation is altered by STS1 and/or STS2. First, we determined that FLT3 and KIT bind to STS1 and STS2 in a ligand-dependent manner in co-immunoprecipitation experiments (Figures 4A and 4B). Because STS1 has been shown to exhibit phosphatase activity through its PGM domain, we analyzed the phosphorylation of FLT3

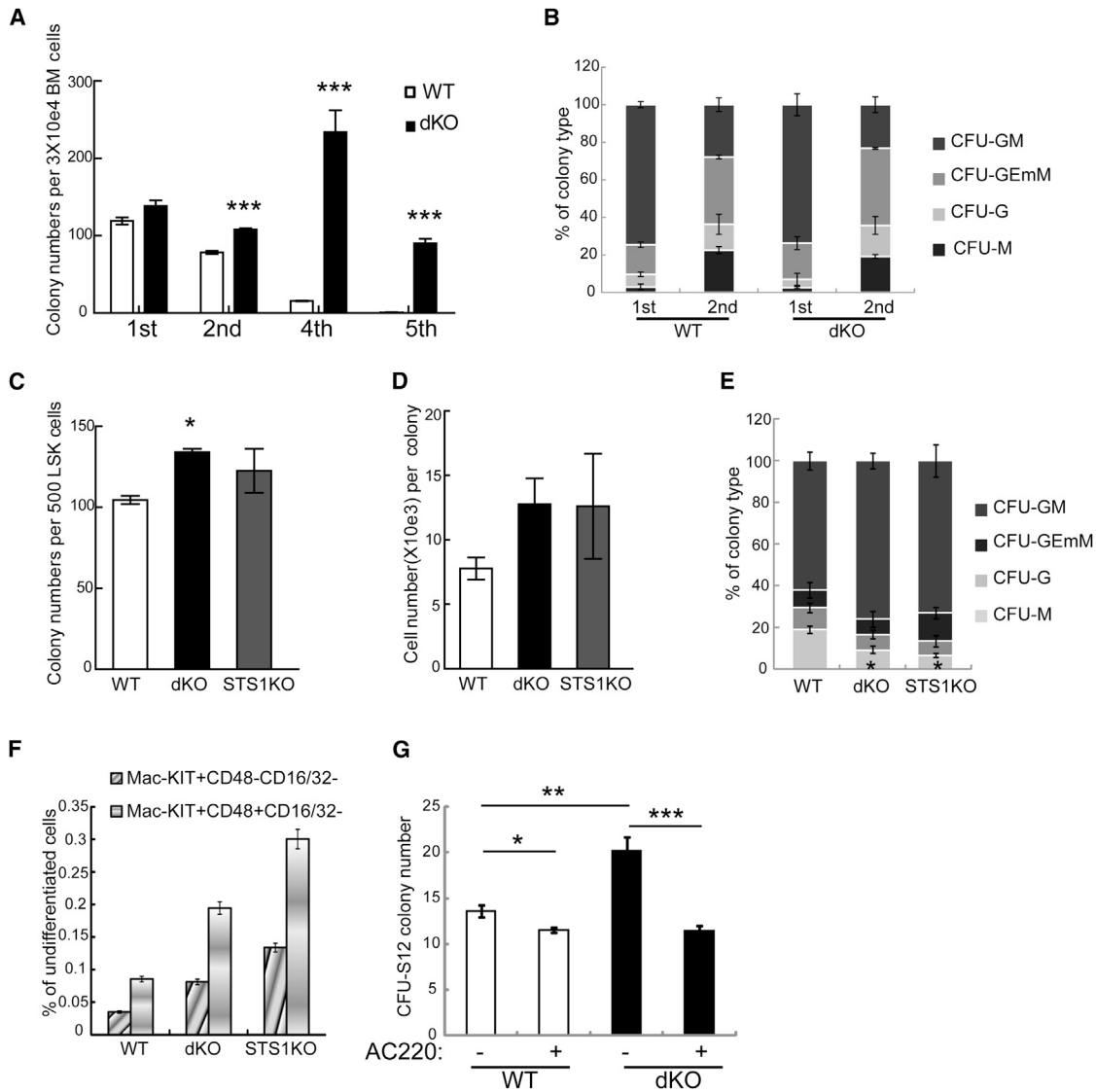


Figure 2. Increased Colony-Forming Ability of STS1/STS2-Deficient Bone Marrow Cells In Vitro and In Vivo

(A) Colony numbers formed in methylcellulose containing IL3, IL6, SCF, and EPO (Methocult 3434). Bone marrow cells were pooled from five dKO and five WT mice. Colonies were replated serially five times, each time in triplicate. Data represent mean \pm SEM. *** p < 0.001.

(B) Morphological assessment of colonies from (A) as percentage of total colonies.

(C) Colony numbers formed by 500 sorted LSK cells from WT (white bar), dKO (black bar), and STS1KO (dark gray) mice. Data represent mean \pm SEM of triplicate experiments. * p < 0.01.

(D) Cell numbers per colony were calculated from the experiment shown in (C). Data represent mean \pm SEM.

(E) Morphological assessment of colonies from (C) as percentage of total colonies. Data represent mean \pm SEM.

(F) Cells from colonies formed by LSK cells (as in B and C) were stained with the surface markers KIT, CD48, CD16/32, and MAC-1, followed by FACS analysis.

(G) Colony-forming units of spleen (CFU-S12) at 12 days post-transplantation of 1×10^5 bone marrow cells into lethally irradiated recipient mice ($n = 5$ in WT, $n = 6$ in dKO, $n = 4$ in WT+AC220, and $n = 5$ in dKO + AC220). Mice were treated daily by oral gavage with vehicle or AC220. * p < 0.05, ** p < 0.01, *** p < 0.001 (Student's *t* test).

(Figure 4C) and KIT (Figure 4D) in the presence of overexpressed STS1 and STS2 or their phosphatase-defective mutants (PGM*) (Mikhailik et al., 2007; Raguz et al., 2007). As shown in Figures 4C and 4D, overexpression of STS1,

but not STS2, led to a reduction of ligand-induced phosphorylation of both FLT3 and KIT. This was dependent on the functional phosphatase domain (PGM) of STS1 because no difference was observed with PGM*. In a reverse

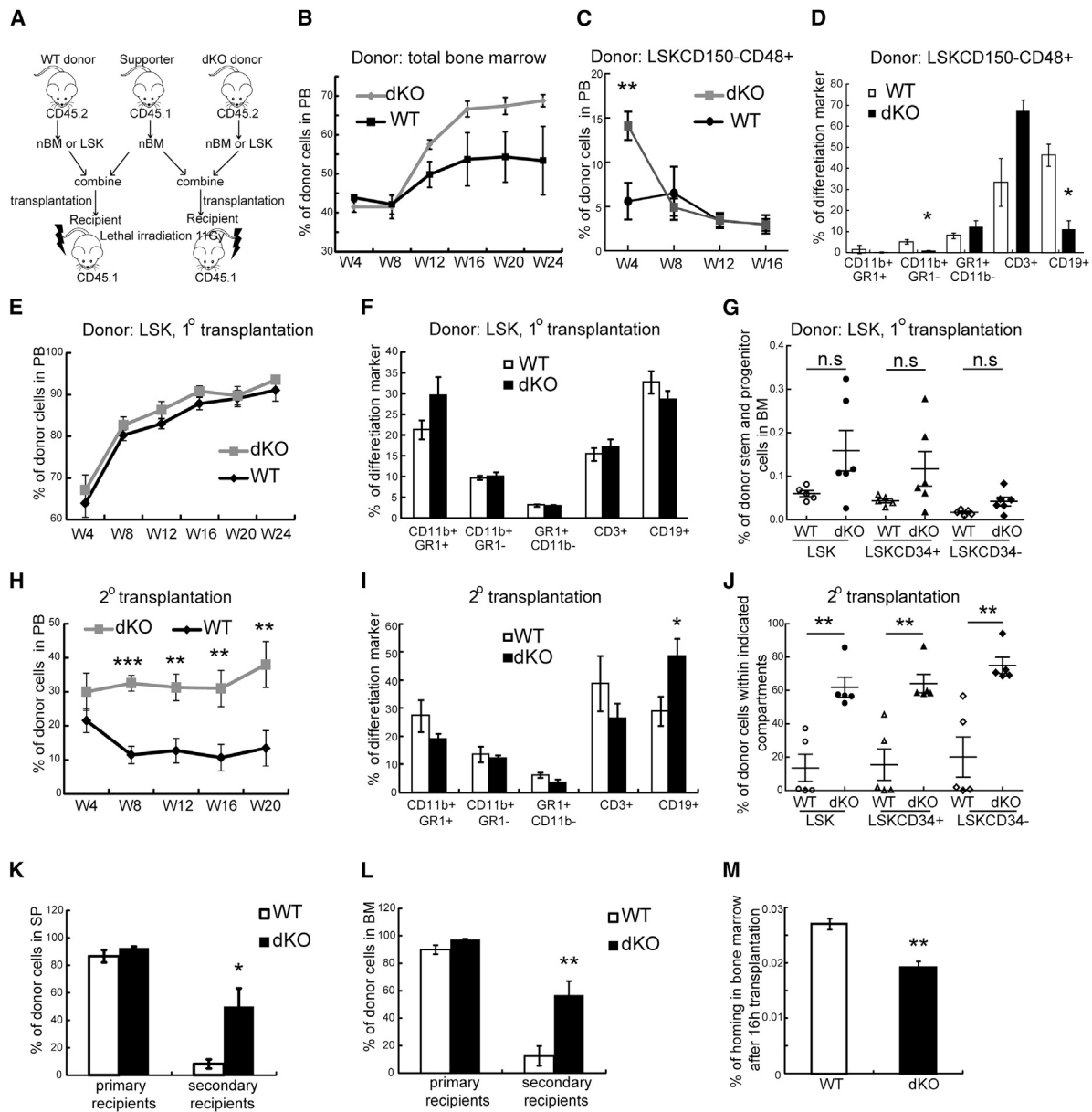


Figure 3. Enhanced Long-Term Repopulation Capacity of dKO HSCs

(A) Schematic of the competitive repopulation assays. Total bone marrow cells or sorted LSK cells from WT or dKO mice (CD45.2⁺) were mixed with competitor WT bone marrow cells (CD45.1⁺). Mixed cells were transplanted intravenously into lethally irradiated (11 Gy) congenic (CD45.1⁺) recipients (n = 10/group).

(B) Long-term repopulation assay using total bone marrow cells as the donor. Recipient mice (n = 10/group) were transplanted with 2 × 10⁶ total bone marrow cells from five WT (white bar) or dKO (black bar) donors (CD45.2⁺) mixed with the same number of WT bone marrow cells as competitors (CD45.1⁺). Data were obtained every 4 weeks (W) by analyzing peripheral blood for CD45.2⁺ donor cells.

(C) Repopulation assay using sorted LSKCD150⁻CD48⁺ cells as the donor. Recipient mice (n = 6/group) were transplanted with 3,000 sorted LSKCD150⁻CD48⁺ cells from four WT (white bar) or dKO (black bar) mice (CD45.2⁺) mixed with 2 × 10⁵ mononuclear bone marrow cells as supporters (CD45.1⁺). Data were obtained every 4 weeks by analyzing peripheral blood for CD45.2⁺ donor cells.

(D) Percentage of differentiated cells in the peripheral blood 4 weeks after transplantation.

(E) Repopulation assay using sorted LSK cells as the donor. Recipient mice (n = 10/group) were transplanted with 3,000 sorted LSK cells from five WT (white bar) or dKO (black bar) donors (CD45.2⁺) mixed with 2 × 10⁵ mononuclear WT bone marrow cells as competitors (CD45.1⁺). Data were obtained every 4 weeks by analyzing peripheral blood for CD45.2⁺ donor cells.

(F) Percentage of differentiated cells in the peripheral blood 8 weeks after transplantation.

(legend continued on next page)



approach, we made use of short hairpin RNA (shRNA) constructs of STS1 and determined a constitutive, ligand-independent phosphorylation (i.e., activation) of FLT3 as well as a hyperphosphorylation of FLT3 in response to FLT3 ligand (FL) stimulation (Figure 4E; Figure S4). As a consequence, this led to consecutive hyperactivation of AKT (Figure 4E). Furthermore, an enhanced FL-dependent expansion was induced by STS1 knock-down in an FLT3-expressing 32D myeloid cell line. This was prevented by the application of a specific FLT3 inhibitor, AC220 (Taylor et al., 2012; Zarrinkar et al., 2009), demonstrating that cell growth depends on FLT3 kinase activity (Figure 4F).

Hyperphosphorylation of FLT3 in dKO Mice Results in a Proliferative Advantage of LSK Cells

Next we aimed to monitor the phosphorylation and signaling events in our genetic mouse model. Lin⁻ bone marrow cells were used for intracellular staining with p-FLT3 antibody. Interestingly, dKO cells showed a significantly higher p-FLT3 signal compared with the WT in the absence of FL stimulation in Lin⁻, LSK, and Lin⁻KIT⁺SCA⁻ (LKSCA⁻) cell populations (Figure 5A, top), suggesting constitutive FLT3 activation. This was also observed in STS1KO and, to a lesser extent, in STS2KO cells (Figure S5A). This difference was abolished by the addition of FL, leading to equal p-FLT3 signals of WT, dKO, and single KO cells (Figure 5A; Figure S5A, bottom). Analysis of the downstream signaling events in Lin⁻ bone marrow cells revealed a higher AKT phosphorylation in dKO and STS1KO mice compared with the WT (Figure 5B).

We then asked whether the constitutive activation of FLT3 in dKO is responsible for the LSK expansion (Figure 1). When purified LSK cells were cultured ex vivo in the presence of SCF and TPO, we observed a faster cell proliferation of dKO LSK cells compared with the WT (Figure 5C, straight line). However, the effect was reversed upon FL stimulation, with an identical expansion curve between the analyzed genotypes (Figure 5C, dotted line). Application of the FLT3 in-

hibitor AC220 reduced cell expansion to the same level (Figure 5C, dashed line). No block in differentiation was determined under these conditions (Figures S5B–S5E).

To further confirm the effect of STS1 and STS2 on cell proliferation, LSKCD48⁻ cells were labeled with a cell proliferation tracker, which allows FACS tracing over multiple generations by measuring the dye dilution. Labeled dKO cells showed an accelerated dilution of the proliferation tracker in the presence of SCF and TPO (i.e., faster cell division) compared with the WT (Figure 5D, left). However, when FL or AC220 were added, the dilution of the fluorescent dye was similar in dKO and WT cells (Figure 5D, center and right), suggesting that the growth advantage of dKO cells is at least partially caused by FLT3 kinase activity.

In summary, these data indicate that depletion of STS1/STS2 causes a constitutive phosphorylation of FLT3 and hyperactivation of downstream AKT signaling, which results in elevated ex vivo LSK cell expansion.

Accelerated Recovery of Hematopoietic Stem and Progenitor Cells in STS1/STS2-Deficient Mice after Cytotoxic Stress In Vivo

We asked whether the enlarged LSK population in dKO mice is due to increased proliferation in vivo. Bromodeoxyuridine (BrdU) incorporation was analyzed in different compartments, but no significant changes were observed (Figure 6A). Next we assessed the quiescence status by Ki67 staining because Ki67 is a nuclear protein expressed in active cycling cells (G1/S/G2/M) and absent in resting cells (G0). No difference was evident under homeostatic conditions (Figure 6B). Apoptosis in distinct bone marrow compartments showed no differences between genotypes (Figure 6C). We then challenged hematopoiesis by a single 5-fluorouracil (5-FU) injection, which causes cytotoxicity to all actively cycling cells, resulting in ablation of the proliferating progenitor pool and sparing only quiescent (stem) cells (Venezia et al., 2004; Wilson et al., 2008, 2009). Analyses of the bone marrow composition after 5-FU injection indicate that there is a continuous increase

(G) Total bone marrow cells from first-transplantation hosts (shown in D) were isolated (from WT, n = 5; from dKO, n = 6) and stained for cell surface markers. The donor LSK, LSKCD34⁺, and LSKCD34⁻ cell frequency in total bone marrow is shown for each mouse.

(H) Total bone marrow cells were isolated from first-transplantation hosts (shown in D and E) and retransplanted into secondary (2°) recipients. For each transplantation, 5 × 10⁵ bone marrow cells from the primary hosts plus an equal number of supporter cells (CD45.1) were transplanted. Data were obtained every 4 weeks by analyzing peripheral blood for CD45.2⁺ donor cells (n = 10/group).

(I) Percentage of differentiated cells in the peripheral blood 8 weeks after transplantation.

(J) Total bone marrow cells from the second transplantation (shown in F, n = 5/group) were isolated and stained for surface markers. The donor cell percentage in Lin⁻, LSK, Lin⁻KIT⁺SCA⁻ compartments is shown for each mouse.

(K) Engraftment of WT or dKO LSK donor cells (CD45.2⁺) in primary and secondary recipients in the spleen (SP) (n = 10/group).

(L) Engraftment of WT or dKO LSK c donor cells (CD45.2⁺) in primary and secondary recipients in BM (n = 10/group).

(M) Homing of WT and dKO Lin⁻ donor cells in recipients' bone marrow (n = 4/group). Lineage-negative bone marrow cells were labeled and transplanted into lethally irradiated recipient mice. These mice were sacrificed after 16 hr to isolate their bone marrow, followed by FACS analysis.

*p < 0.05, **p < 0.01, ***p < 0.001. Data represent the mean ± SEM. See also Figure S3.

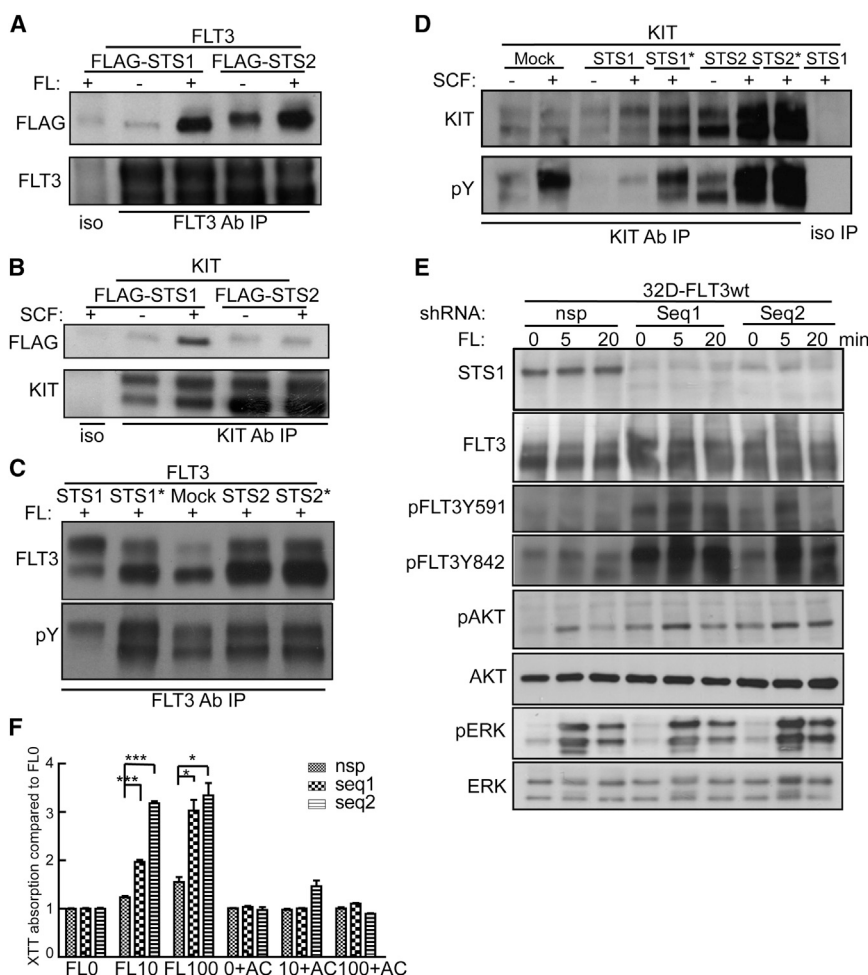


Figure 4. STS1/STS2 Interact with FLT3/KIT and Function as Phosphatases

(A) 293T cells were transiently transfected with FLT3 and FLAG-tagged STS1 or STS2 constructs. Cells were serum-starved overnight and then stimulated for 10 min at 37°C with 40 ng/ml FL. FLT3 was immunoprecipitated, and co-IP of STS1/STS2 was detected by immunoblotting. IP, immunoprecipitation; iso, normal rabbit antibody; Ab, antibody.

(B) 293T cells were co-transfected with KIT and FLAG-tagged STS1 or STS2 constructs. Cells were serum-starved and stimulated with KIT ligand (SCF 40 ng/ml) for 10 min. KIT was immunoprecipitated and co-IP of STS1/STS2 was detected by immunoblotting.

(C) Phosphatase activity of STS proteins on FLT3 was analyzed by co-expression of FLT3 and the respective STS constructs. FLT3 and FLAG-tagged STS1/STS2 or their PGM domain point mutants STS1* and STS2* were transiently transfected into 293T cells. Cells were serum-starved and stimulated with FL (40 ng/ml) for 10 min. FLT3 was immunoprecipitated and detected with anti-FLT3 and pan-pY antibody (4G10).

(D) Phosphatase activity of STS proteins on KIT was analyzed by co-expression of KIT and the respective STS constructs. Cells were serum-starved and stimulated with SCF (40 ng/ml) for 10 min. KIT was immunoprecipitated. Total KIT and pan-pY were detected by immunoblotting.

(E) 32D cells stably expressing FLT3WT were transfected with shRNA against STS1 (Seq1 and Seq2) or a non-specific sequence (nsp) and stimulated with FL (100 ng/ml) for different times after serum and cytokine starvation. FLT3 phosphorylation and downstream signaling were detected by western blot.

(F) The influence of STS1 knockdown on 32D-FLT3WT cell growth was measured by 2,3-bis-(2-methoxy-4-nitro-5-sulfophenyl)-2H-tetrazolium-5-carboxanilide (XTT) assay. XTT absorption was measured after 48 hr in the absence (FL 0) or presence of FLT3 ligand: 10 ng/ml (FL10) and 100 ng/ml (FL100) with or without the kinase inhibitor AC220 (20 nM) (+AC).

Data are mean ± SEM (n = 3 experiments). See also Figure S4.

of the stem and progenitor populations and Ki67⁺ cells from days 3–7, indicating a gradual recovery of these populations (Figures S6A and S6B). By analyzing the cell-cycle status by Ki67 and 7-aminoactinomycin D (7AAD) staining, dKO mice show a larger population of proliferating cells (S/G2/M) and fewer quiescent cells (in G0 phase) within both the LSK and HSC (LSK CD150⁺CD48⁻) compartments on day 6 after 5-FU injection (Figures 6D and 6E). These data suggest that dKO bone marrow cells exit G0 and divide faster after 5-FU-induced myeloablation (Figures 6D and 6E). Consistently, STS1/STS2-deficient mice showed an improved recovery in white blood cells (WBCs) compared with the WT (day 7 onward; Figure 6F).

More cells were produced by dKO when equal bone marrow cells from day 8 after single 5FU injection were seeded for colony assays (Figure 6G, right). In a detailed immunophenotype analysis, mice lacking STS1/STS2 also demonstrated enhanced recovery of LSK populations on day 8, which was especially prominent in the LSKCD48⁺ compartment (Figure 6H), although both the dKO and WT groups showed a similar loss of KIT⁺ cells on day 2 (Figure S6C).

In summary, the data demonstrate that, after 5-FU cytotoxic injury, the quiescent HSCs from dKO mice cycle and proliferate faster and show enhanced recovery compared with their WT controls.

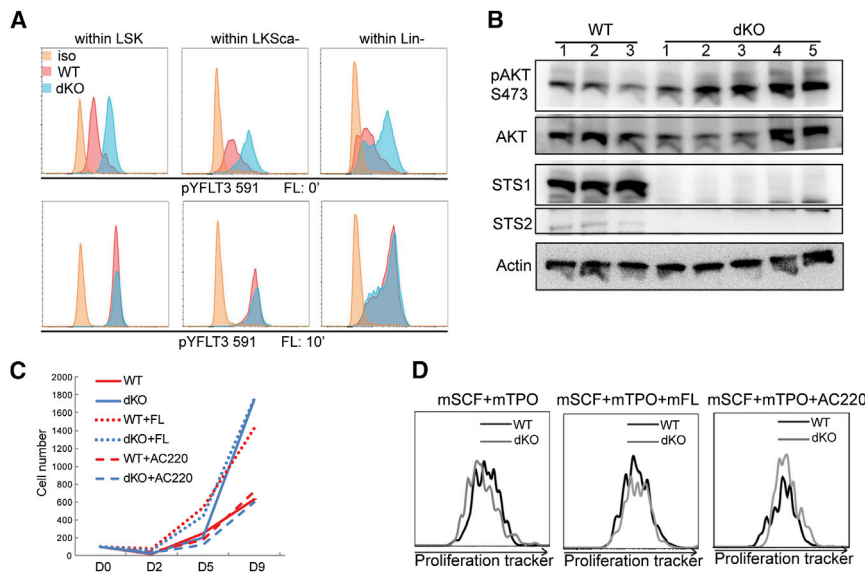


Figure 5. Hyperphosphorylation of FLT3 and Faster Ex Vivo Proliferation of dKO LSK

(A) Intracellular staining of pY591-FLT3 with (FL 10') or without (FL 0') FLT3 ligand stimulation in Lin⁻ bone marrow cells from WT (red) and dKO (blue) mice. Cells were gated on different compartments, and FLT3 phosphorylation on pY591 is shown. Data are representative of three independent experiments.

(B) Lin⁻ bone marrow cells were isolated from WT and dKO mice and used for immunoblotting. Data are representative of four independent experiments.

(C) LSK cells were sorted and ex vivo-cultured in serum-free medium in the presence of different cytokines or the FLT3-inhibitor AC220. Data are representative of four independent experiments.

(D) LSKCD48⁻ cells were sorted, labeled with proliferation tracker violet, and cultured ex vivo in serum-free medium under the indicated conditions. The dilution of the proliferation tracker was measured after 4 days. Data are representative of two independent experiments. See also Figure S5.

DISCUSSION

FLT3 and KIT are key RTKs controlling HSPCs. Ubiquitination and dephosphorylation are two important mechanisms to negatively regulate RTK signaling (Dikic and Giordano, 2003; Sastry and Elferink, 2011).

By using single- and double-knockout mice, our data demonstrate that loss of both STS1/STS2 causes a remarkable expansion of the MPP and LMPP cell populations. Consistently, functional analyses demonstrated increased colony-forming ability and a strong but transient engraftment advantage after transplantation of sorted LMPPs, suggesting enhanced multipotent progenitor cell fitness. Surprisingly, although HSCs were not increased in number, competitive repopulation assays demonstrated that dKO mice display a dramatically elevated long-term repopulation capacity after serial transplantation. Because the LMPP transplantation did not provide evidence of long-term repopulation capacity from these progenitor cells, our data indicate that HSCs lacking STS1/STS2 have superior fitness and efficiently replenish the MPP and LMPP pools. Of note, with increasing age, the LSK compartment of dKO mice amplifies, which provides further circumstantial evidence of improved HSC fitness.

The functional analyses demonstrated that increased proliferation and increased cell fitness account for the phenotype upon loss of STS1/STS2, whereas we found no evidence of increased bone marrow homing, reduced apoptosis, or blocked differentiation. Although we cannot fully exclude non-cell autonomous effects, the significantly increased hematopoietic stem and progenitor cell

expansion of dKO cells after secondary transplantation strongly argue in favor of a direct cell-autonomous effect of STS1/STS2 loss on HSCs and multipotent progenitor cells.

These data are in agreement with observations made in CBL and Itch knockout mice, which show a significant expansion of HSCs, MPPs, and LMPPs upon serial transplantation and under stress conditions (Heidel et al., 2013; Rathinam et al., 2008, 2011). Interestingly, our data revealed that the increased LSK compartment in STS1/STS2 dKO mice is mainly restricted to the expansion of MPP and LMPP subpopulations, with no phenotypic expansion of HSCs. The difference from CBL and Itch knockout mice may be due to the fact that these E3 ligases affect more signaling molecules and pathways (Schmidt and Dikic, 2005), whereas STS1/STS2 may have more specific functions and binding partners.

At the molecular level, our data demonstrate that the growth advantage of dKO HSPCs is largely dependent on increased FLT3 kinase activity (with subsequent constitutive AKT activation) and can be prevented by FLT3 inhibition. Consistently, a recent publication regarding FLT3 knockout mice has shown that FLT3 deficiency impaired the expansion of multipotent progenitor cells, thereby blocking the generation of both lymphoid and myeloid progenitors (Beaudin et al., 2014).

Importantly, our findings suggest that STS1/STS2 function is important under stress conditions in HSPCs after transplantation. On the contrary, under steady-state conditions, the role of STS1/STS2 is dispensable. Similarly, the effects of FLT3 deficiency on the generation of all mature

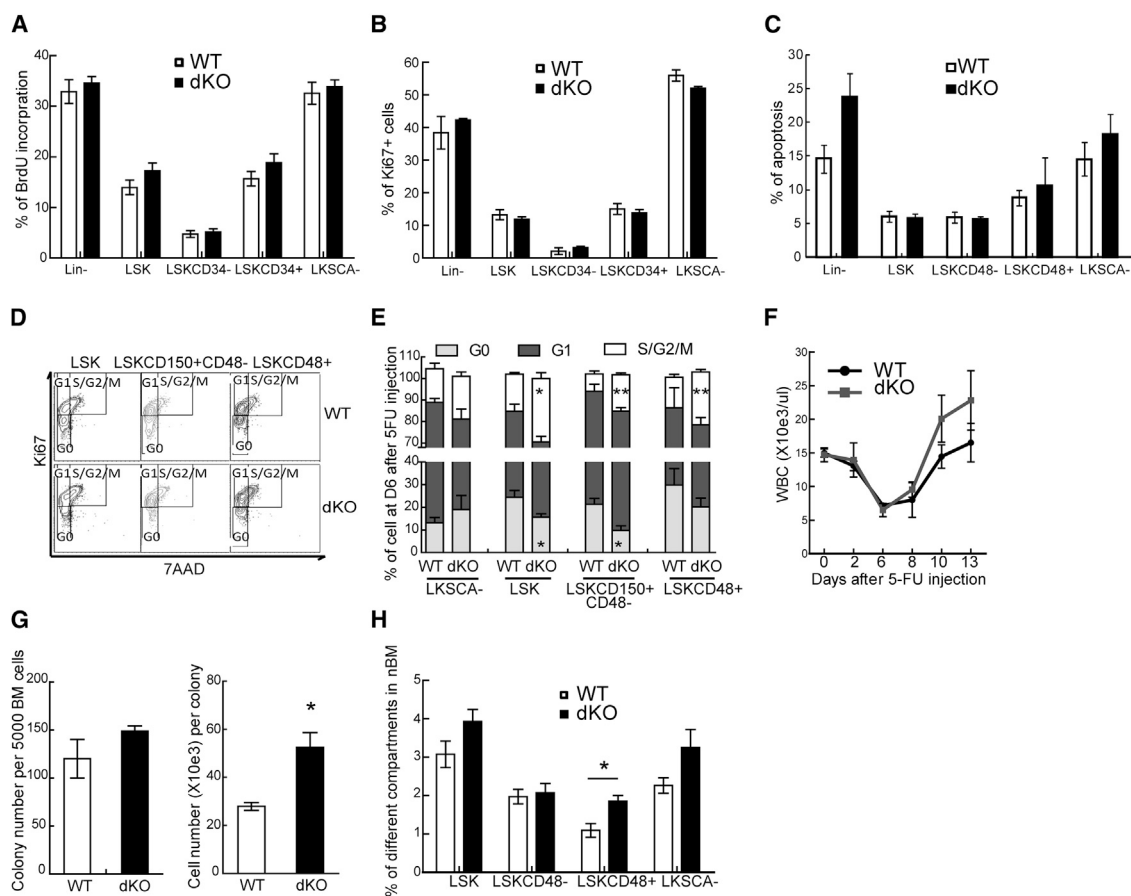


Figure 6. Accelerated Hematopoietic Recovery of dKO Mice after Cytotoxic Stress In Vivo

(A) BrdU incorporation in different bone marrow compartments at steady state (n = 5/group).
 (B) Ki67⁺ cell percentage in different bone marrow compartments at steady state (WT, n = 5; dKO, n = 6).
 (C) Percentage of apoptotic cells (as percent Annexin V⁺) in different bone marrow compartments (n = 5/group).
 (D) Representative FACS plots of cell-cycle status based on Ki67 and 7AAD staining in LSK, LSKCD150⁺CD48⁻, and LSKCD48⁺ compartments on day 6 after 5-FU injection.
 (E) Cell-cycle status on day 6 after a single 5-FU injection (as shown in D; WT, n = 4; dKO, n = 3).
 (F) WBC counts on different days after a single 5-FU injection (WT, n = 4; dKO, n = 5).
 (G) Colony numbers formed by 5,000 total bone marrow cells from WT/dKO mice 8 days after 5-FU injection (left). Also shown are cell numbers per colony (right). Data are mean ± SEM (n = 3 experiments).
 (H) Distribution of HSPC compartments in WT and dKO total BM (n = 7/group) on day 8 after a single 5-FU injection. Data represent mean ± SEM.

See also [Figure S6](#).

lineages are only detectable after transplantation of purified progenitors (Beaudin et al., 2014). The constitutive activation of FLT3 in our STS1/STS2 dKO model causes neither HSC exhaustion nor leukemia development as in the CBL or Itch KO model (Heidel et al., 2013; Rathinam et al., 2008, 2011). On the contrary, previous reports of work with the oncogenic mutant FLT3-ITD have found defective HSC function (Adolfsson et al., 2001; Chu et al., 2012). However, FLT3-ITD expression differs from WT-FLT3 in many aspects, including strong activation of STAT5 and a subcellular localization to the ER, which alters

signaling qualities and receptor trafficking (Choudhary et al., 2007, 2009). Therefore, numerous biological properties of FLT3-ITD account for the difference to our dKO phenotype.

As reported, FLT3 is mainly expressed on progenitor cells in mice, and both FLT3 and its ligand FL are dispensable for HSC maintenance and post-transplantation expansion (Adolfsson et al., 2005; Boyer et al., 2011; Buza-Vidas et al., 2009). In contrast, KIT plays an essential role in regulating HSC self-renewal and cell quiescence (Sharma et al., 2007; Thorén et al., 2008). Interestingly, STS1 showed



phosphatase activity on both FLT3 and KIT in vitro. Although we only detected hyperphosphorylation of FLT3 (but not KIT) in primary dKO cells, we cannot exclude limitations of reagents to detect phospho-KIT. Therefore, we postulate that, in dKO mice, increased KIT activity may be responsible for enhanced HSC fitness. Nevertheless, the basal level of FLT3 expression (mRNA and intracellular protein) is also detectable in long-term engrafting SLAM cells (Chu et al., 2012), suggesting a possible mechanism of STS1/STS2 affecting HSC via FLT3. Furthermore, we cannot exclude that STS1/STS2 may have additional phosphatase substrates contributing to the hematological phenotype.

Interestingly, we observed increased cell-cycle entry and faster cell-cycle progression after 5-FU injection in dKO HSCs, indicating that STS1/STS2 might also be involved in cell-cycle regulation. Because the cell cycle is tightly controlled by the phosphorylation of several regulators (Kalaszczynska et al., 2009; Pietras et al., 2011), it can be speculated that some of these regulators may be STS1/STS2 phosphatase substrates.

Importantly, STS1 and STS2 have been shown to have overlapping functions (Carpino et al., 2002; Carpino et al., 2004). However, although expansion of LSK, increased serial colony growth, and hyperphosphorylation of FLT3 were largely attributable to the loss of STS1, further loss of STS2 strengthened the phenotype, and depletion of STS2 showed in vivo phosphatase activity as well. Because STS1 and STS2 differ in their substrate specificity (Chen et al., 2009a, 2009b) and their expression pattern differs in hematopoiesis, we suspect that subtle functional differences exist between STS1 and STS2.

Studies on several other phosphatases, such as SHP2, PRL2, PTP σ , and PTP ζ , indicate a frequent involvement of phosphatases in HSC regulation. Among these, PTP σ and PTP ζ are transmembrane receptor tyrosine phosphatases. Knockout of these proteins augments HSC function. However, their effects are non-autonomous and are rather due to their interaction with the bone marrow microenvironment (Himburg et al., 2012; Quarmyne et al., 2015). SHP2 and PRL2 are both intra-cytoplasmic phosphatases and have been shown to increase HSC self-renewal as opposed to STS1/STS2 (Chan et al., 2011; Kobayashi et al., 2014; Zhu et al., 2011). None of the phosphatases (SHP2, PRL2, PTP σ , and PTP ζ) have been reported to directly dephosphorylate RTKs.

In summary, we elucidated that (1) dKO mice display phenotypic expansion and increased fitness of MPPs and LMPPs; (2) HSCs lacking STS1/STS2 exhibit improved fitness; and (3) STS1/STS2 are direct phosphatases of FLT3 and KIT. Our data imply that phosphatase inhibition of STS1 and STS2 may potentially improve hematopoietic recovery after bone marrow transplantation, opening new venues for therapeutic intervention.

EXPERIMENTAL PROCEDURES

Reagents and Antibodies

Recombinant human and murine cytokines were purchased from PeproTech. Methylcellulose (MethoCult 3630, catalog no. 3434) was purchased from STEMCELL Technologies. All antibody information is summarized in Table S1.

Mice

STS1 and STS2 dKO mice have been reported previously and were backcrossed for 10 generations onto the C57BL6 background (Carpino et al., 2002, 2004). The dKO mice were crossed with wild-type C57BL6 mice to generate STS1^{-/-} and STS2^{-/-} single-knockout mice. All mice were kept under specific pathogen-free conditions in the animal care facility. Mouse experiments were approved by the local animal experimentation committee.

Cell Lines

The 32Dcl3 and 293T cell lines were cultured as described previously (Bandi et al., 2009; Sargin et al., 2007). The stable 32D-FLT3 cell line was generated by retroviral transduction with human FLT3WT. For STS1 knockdown experiments, stable 32D-FLT3 cell lines were infected lentivirally with pLKO.1-STS1-shRNA (sequences 1 and 2) or non-specific shRNA (nsp) from Sigma Aldrich.

Flow Cytometry

Single-cell suspensions were measured on flow cytometers: FACSFortessa or FACSCanto II (BD Biosciences). FACSDiva software (BD Biosciences) or FlowJo software (Tree Star) were used for data analyses. Cells were sorted into defined subpopulations with a FACSAria II (BD Biosciences). Total or lineage-negative bone marrow cells were stained and gated according to established methods (Kiel et al., 2005; Oguro et al., 2013; Rathinam et al., 2008, 2011; Yamamoto et al., 2013; Yilmaz et al., 2006). For the CLP assay, total bone marrow cells were stained with a lineage cocktail (CD3, CD11b, GR1, and TER119) and B220 with separate fluorochromes (Karsunky et al., 2008). Isotype antibodies were used as negative controls for FACS gating.

Homing Assay

Lineage-depleted WT or dKO bone marrow cells were labeled with CellTrace carboxyfluorescein succinimidyl ester (CFSE) (Life Technologies), and 5X10⁵ cells were transplanted into lethally irradiated recipients. 16 hr later, recipients were sacrificed, and the percentage of CFSE⁺ cells in total bone marrow was analyzed by FACS.

Competitive Repopulation Assays and Bone Marrow Transplantation Studies

For competitive repopulation experiments, total bone marrow, sorted LSKCD150⁻CD48⁺ cells, or LSK cells from wild-type or dKO mice (CD45.2⁺) were mixed with competitor bone marrow cells (CD45.1⁺). The mixed cells were transplanted intravenously into lethally irradiated (11 Gy) congenic (CD45.1⁺) recipients.

Mice were bled every 4 weeks. The donor cell percentage and distribution of the myeloid or lymphoid populations were analyzed by FACS.



Colony-Forming Unit Assays

For colony-forming unit assays, 3×10^4 mononucleated bone marrow cells or 500 sorted LSK cells were cultured in semisolid methylcellulose (containing IL3, IL6, SCF, and EPO). Colonies were scored according to the manufacturer's instructions. Cells were collected and replated several times.

For CFU-S assays, 100,000 mononucleated bone marrow cells from WT or dKO mice were injected into lethally irradiated recipient WT mice. The recipient mice were given vehicle or 10 mg/kg AC220 (in 0.5% methylcellulose) by oral gavage for 11 days (Taylor et al., 2012). Mice were sacrificed on day 12, and colony numbers were counted on the spleen surface.

Treatment with BrdU or 5-FU

Mice were given a single intraperitoneal dose of BrdU (1 mg) or 5-FU (150 mg/kg body weight) and sacrificed at the indicated times. Peripheral blood counts were measured by Hemavet.

ACCESSION NUMBERS

The accession numbers for the human STS1 and STS2 sequences used for in vitro expression are GenBank: NM_032873.4, NM_001001895.

SUPPLEMENTAL INFORMATION

Supplemental Information includes six figures and one table and can be found with this article online at <http://dx.doi.org/10.1016/j.stemcr.2015.08.006>.

AUTHOR CONTRIBUTIONS

J.Z. and C.B. designed the research and analyzed the data. J.Z., O.V., S.R.B., Ö.D., J.U.K., R.G.F., K.J., and A.E. performed the experiments. J.Z., L.R., N.C., M.R., H.S., and C.B. interpreted the results and discussed the data. J.Z. and C.B. wrote the manuscript.

ACKNOWLEDGMENTS

We wish to thank Frank Böhmer and Jörg Müller for numerous helpful experimental suggestions and careful reading of the manuscript. We also thank Daniela Höller for reagents and initial planning of the experiments. The authors thank Deutsche José Carreras Leukämie-Stiftung (grant DJCLS F 10/03 to J.Z.), the German Cancer Aid (Deutsche Krebshilfe, 108688 and 108400, to C.H.B) and LOEWE (IIL4-518/17.004 [2010] and IIL6-518/75.004 [2013], to C.H.B.).

Received: January 28, 2015

Revised: August 5, 2015

Accepted: August 6, 2015

Published: September 10, 2015

REFERENCES

Adolfsson, J., Borge, O.J., Bryder, D., Theilgaard-Mönch, K., Asstrand-Grundström, I., Sitnicka, E., Sasaki, Y., and Jacobsen, S.E. (2001). Upregulation of Flt3 expression within the bone marrow

Lin(-)Sca1(+)c-kit(+) stem cell compartment is accompanied by loss of self-renewal capacity. *Immunity* 15, 659–669.

Adolfsson, J., Månsson, R., Buza-Vidas, N., Hultquist, A., Liuba, K., Jensen, C.T., Bryder, D., Yang, L., Borge, O.J., Thoren, L.A., et al. (2005). Identification of Flt3+ lympho-myeloid stem cells lacking erythro-megakaryocytic potential a revised road map for adult blood lineage commitment. *Cell* 121, 295–306.

Bandi, S.R., Brandts, C., Rensinghoff, M., Grundler, R., Tickenbrock, L., Köhler, G., Duyster, J., Berdel, W.E., Müller-Tidow, C., Serve, H., and Sargin, B.; Study Alliance Leukemias (2009). E3 ligase-defective Cbl mutants lead to a generalized mastocytosis and myeloproliferative disease. *Blood* 114, 4197–4208.

Beaudin, A.E., Boyer, S.W., and Forsberg, E.C. (2014). Flk2/Flt3 promotes both myeloid and lymphoid development by expanding non-self-renewing multipotent hematopoietic progenitor cells. *Exp. Hematol.* 42, 218–229.e4.

Boyer, S.W., Schroeder, A.V., Smith-Berdan, S., and Forsberg, E.C. (2011). All hematopoietic cells develop from hematopoietic stem cells through Flk2/Flt3-positive progenitor cells. *Cell Stem Cell* 9, 64–73.

Buza-Vidas, N., Cheng, M., Duarte, S., Charoudeh, H.N., Jacobsen, S.E.W., and Sitnicka, E. (2009). FLT3 receptor and ligand are dispensable for maintenance and posttransplantation expansion of mouse hematopoietic stem cells. *Blood* 113, 3453–3460.

Carpino, N., Kobayashi, R., Zang, H., Takahashi, Y., Jou, S.-T., Feng, J., Nakajima, H., and Ihle, J.N. (2002). Identification, cDNA cloning, and targeted deletion of p70, a novel, ubiquitously expressed SH3 domain-containing protein. *Mol. Cell. Biol.* 22, 7491–7500.

Carpino, N., Turner, S., Mekala, D., Takahashi, Y., Zang, H., Geiger, T.L., Doherty, P., and Ihle, J.N. (2004). Regulation of ZAP-70 activation and TCR signaling by two related proteins, Sts-1 and Sts-2. *Immunity* 20, 37–46.

Carpino, N., Chen, Y., Nassar, N., and Oh, H.-W. (2009). The Sts proteins target tyrosine phosphorylated, ubiquitinated proteins within TCR signaling pathways. *Mol. Immunol.* 46, 3224–3231.

Chan, G., Cheung, L.S., Yang, W., Milyavsky, M., Sanders, A.D., Gu, S., Hong, W.X., Liu, A.X., Wang, X., Barbara, M., et al. (2011). Essential role for Ptpn11 in survival of hematopoietic stem and progenitor cells. *Blood* 117, 4253–4261.

Chen, Y., Jakoncic, J., Carpino, N., and Nassar, N. (2009a). Structural and functional characterization of the 2H-phosphatase domain of Sts-2 reveals an acid-dependent phosphatase activity. *Biochemistry* 48, 1681–1690.

Chen, Y., Jakoncic, J., Parker, K.A., Carpino, N., and Nassar, N. (2009b). Structures of the phosphorylated and VO(3)-bound 2H-phosphatase domain of Sts-2. *Biochemistry* 48, 8129–8135.

Choudhary, C., Brandts, C., Schwable, J., Tickenbrock, L., Sargin, B., Ueker, A., Böhmer, F.D., Berdel, W.E., Müller-Tidow, C., and Serve, H. (2007). Activation mechanisms of STAT5 by oncogenic Flt3-ITD. *Blood* 110, 370–374.

Choudhary, C., Olsen, J.V., Brandts, C., Cox, J., Reddy, P.N., Böhmer, F.D., Gerke, V., Schmidt-Arras, D.E., Berdel, W.E., Müller-Tidow, C., et al. (2009). Mislocalized activation of oncogenic RTKs switches downstream signaling outcomes. *Mol. Cell* 36, 326–339.



- Chu, S.H., Heiser, D., Li, L., Kaplan, I., Collector, M., Huso, D., Sharkey, S.J., Civin, C., and Small, D. (2012). FLT3-ITD knockin impairs hematopoietic stem cell quiescence/homeostasis, leading to myeloproliferative neoplasm. *Cell Stem Cell* *11*, 346–358.
- Dikic, I., and Giordano, S. (2003). Negative receptor signalling. *Curr. Opin. Cell Biol.* *15*, 128–135.
- Feshchenko, E.A., Smirnova, E.V., Swaminathan, G., Teckchandani, A.M., Agrawal, R., Band, H., Zhang, X., Annan, R.S., Carr, S.A., and Tsygankov, A.Y. (2004). TULA: an SH3- and UBA-containing protein that binds to c-Cbl and ubiquitin. *Oncogene* *23*, 4690–4706.
- Heidel, F.H., Bullinger, L., Arriba-Tutusa, P., Wang, Z., Gaebel, J., Hirt, C., Niederwieser, D., Lane, S.W., Döhner, K., Vasioukhin, V., et al. (2013). The cell fate determinant Lgl1 influences HSC fitness and prognosis in AML. *J. Exp. Med.* *210*, 15–22.
- Himburg, H.A., Harris, J.R., Ito, T., Daher, P., Russell, J.L., Quarmyne, M., Doan, P.L., Helms, K., Nakamura, M., Fixsen, E., et al. (2012). Pleiotrophin regulates the retention and self-renewal of hematopoietic stem cells in the bone marrow vascular niche. *Cell Rep.* *2*, 964–975.
- Hoeller, D., Crosetto, N., Blagoev, B., Raiborg, C., Tikkanen, R., Wagner, S., Kowanetz, K., Breitling, R., Mann, M., Stenmark, H., and Dikic, I. (2006). Regulation of ubiquitin-binding proteins by monoubiquitination. *Nat. Cell Biol.* *8*, 163–169.
- Kalaszczynska, I., Geng, Y., Iino, T., Mizuno, S., Choi, Y., Kondratyuk, I., Silver, D.P., Wolgemuth, D.J., Akashi, K., and Sicinski, P. (2009). Cyclin A is redundant in fibroblasts but essential in hematopoietic and embryonic stem cells. *Cell* *138*, 352–365.
- Karsunky, H., Inlay, M.A., Serwold, T., Bhattacharya, D., and Weissman, I.L. (2008). Flk2+ common lymphoid progenitors possess equivalent differentiation potential for the B and T lineages. *Blood* *111*, 5562–5570.
- Kiel, M.J., Yilmaz, O.H., Iwashita, T., Yilmaz, O.H., Terhorst, C., and Morrison, S.J. (2005). SLAM family receptors distinguish hematopoietic stem and progenitor cells and reveal endothelial niches for stem cells. *Cell* *121*, 1109–1121.
- Kobayashi, M., Bai, Y., Dong, Y., Yu, H., Chen, S., Gao, R., Zhang, L., Yoder, M.C., Kapur, R., Zhang, Z.Y., and Liu, Y. (2014). PRL2/PTP4A2 phosphatase is important for hematopoietic stem cell self-renewal. *Stem Cells* *32*, 1956–1967.
- Kowanetz, K., Crosetto, N., Haglund, K., Schmidt, M.H.H., Heldin, C.-H., and Dikic, I. (2004). Suppressors of T-cell receptor signaling Sts-1 and Sts-2 bind to Cbl and inhibit endocytosis of receptor tyrosine kinases. *J. Biol. Chem.* *279*, 32786–32795.
- Mackaretschian, K., Hardin, J.D., Moore, K.A., Boast, S., Goff, S.P., and Lemischka, I.R. (1995). Targeted disruption of the flk2/flt3 gene leads to deficiencies in primitive hematopoietic progenitors. *Immunity* *3*, 147–161.
- Mikhailik, A., Ford, B., Keller, J., Chen, Y., Nassar, N., and Carpino, N. (2007). A phosphatase activity of Sts-1 contributes to the suppression of TCR signaling. *Mol. Cell* *27*, 486–497.
- Oguro, H., Ding, L., and Morrison, S.J. (2013). SLAM family markers resolve functionally distinct subpopulations of hematopoietic stem cells and multipotent progenitors. *Cell Stem Cell* *13*, 102–116.
- Pietras, E.M., Warr, M.R., and Passegué, E. (2011). Cell cycle regulation in hematopoietic stem cells. *J. Cell Biol.* *195*, 709–720.
- Quarmyne, M., Doan, P.L., Himburg, H.A., Yan, X., Nakamura, M., Zhao, L., Chao, N.J., and Chute, J.P. (2015). Protein tyrosine phosphatase-σ regulates hematopoietic stem cell-repopulating capacity. *J. Clin. Invest.* *125*, 177–182.
- Raguz, J., Wagner, S., Dikic, I., and Hoeller, D. (2007). Suppressor of T-cell receptor signalling 1 and 2 differentially regulate endocytosis and signalling of receptor tyrosine kinases. *FEBS Lett.* *581*, 4767–4772.
- Rathinam, C., Thien, C.B.F., Langdon, W.Y., Gu, H., and Flavell, R.A. (2008). The E3 ubiquitin ligase c-Cbl restricts development and functions of hematopoietic stem cells. *Genes Dev.* *22*, 992–997.
- Rathinam, C., Thien, C.B., Flavell, R.A., and Langdon, W.Y. (2010). Myeloid leukemia development in c-Cbl RING finger mutant mice is dependent on FLT3 signaling. *Cancer Cell* *18*, 341–352.
- Rathinam, C., Matesic, L.E., and Flavell, R.A. (2011). The E3 ligase Itch is a negative regulator of the homeostasis and function of hematopoietic stem cells. *Nat. Immunol.* *12*, 399–407.
- Rossi, L., Lin, K.K., Boles, N.C., Yang, L., King, K.Y., Jeong, M., Mayle, A., and Goodell, M.A. (2012). Less is more: unveiling the functional core of hematopoietic stem cells through knockout mice. *Cell Stem Cell* *11*, 302–317.
- Ryan, P.E., Davies, G.C., Nau, M.M., and Lipkowitz, S. (2006). Regulating the regulator: negative regulation of Cbl ubiquitin ligases. *Trends Biochem. Sci.* *31*, 79–88.
- Sargin, B., Choudhary, C., Crosetto, N., Schmidt, M.H., Grundler, R., Rensinghoff, M., Thiessen, C., Tickenbrock, L., Schwäble, J., Brandts, C., et al. (2007). Flt3-dependent transformation by inactivating c-Cbl mutations in AML. *Blood* *110*, 1004–1012.
- Sastry, S.K., and Elferink, L.A. (2011). Checks and balances: interplay of RTKs and PTPs in cancer progression. *Biochem. Pharmacol.* *82*, 435–440.
- Schmidt, M.H.H., and Dikic, I. (2005). The Cbl interactome and its functions. *Nat. Rev. Mol. Cell Biol.* *6*, 907–918.
- Sharma, Y., Astle, C.M., and Harrison, D.E. (2007). Heterozygous kit mutants with little or no apparent anemia exhibit large defects in overall hematopoietic stem cell function. *Exp. Hematol.* *35*, 214–220.
- Taylor, S.J., Dagger, S.A., Thien, C.B., Wikstrom, M.E., and Langdon, W.Y. (2012). Flt3 inhibitor AC220 is a potent therapy in a mouse model of myeloproliferative disease driven by enhanced wild-type Flt3 signaling. *Blood* *120*, 4049–4057.
- Thorén, L.A., Liuba, K., Bryder, D., Nygren, J.M., Jensen, C.T., Qian, H., Antonchuk, J., and Jacobsen, S.E. (2008). Kit regulates maintenance of quiescent hematopoietic stem cells. *J. Immunol.* *180*, 2045–2053.
- Toffalini, F., and Demoulin, J.-B. (2010). New insights into the mechanisms of hematopoietic cell transformation by activated receptor tyrosine kinases. *Blood* *116*, 2429–2437.
- Venezia, T.A., Merchant, A.A., Ramos, C.A., Whitehouse, N.L., Young, A.S., Shaw, C.A., and Goodell, M.A. (2004). Molecular signatures of proliferation and quiescence in hematopoietic stem cells. *PLoS Biol.* *2*, e301.



- Verstraete, K., and Savvides, S.N. (2012). Extracellular assembly and activation principles of oncogenic class III receptor tyrosine kinases. *Nat. Rev. Cancer* *12*, 753–766.
- Wilson, A., Laurenti, E., Oser, G., van der Wath, R.C., Blanco-Bose, W., Jaworski, M., Offner, S., Dunant, C.F., Eshkind, L., Bockamp, E., et al. (2008). Hematopoietic stem cells reversibly switch from dormancy to self-renewal during homeostasis and repair. *Cell* *135*, 1118–1129.
- Wilson, A., Laurenti, E., and Trumpp, A. (2009). Balancing dormant and self-renewing hematopoietic stem cells. *Curr. Opin. Genet. Dev.* *19*, 461–468.
- Yamamoto, R., Morita, Y., Ooehara, J., Hamanaka, S., Onodera, M., Rudolph, K.L., Ema, H., and Nakauchi, H. (2013). Clonal analysis unveils self-renewing lineage-restricted progenitors generated directly from hematopoietic stem cells. *Cell* *154*, 1112–1126.
- Yilmaz, O.H., Kiel, M.J., and Morrison, S.J. (2006). SLAM family markers are conserved among hematopoietic stem cells from old and reconstituted mice and markedly increase their purity. *Blood* *107*, 924–930.
- Zarrinkar, P.P., Gunawardane, R.N., Cramer, M.D., Gardner, M.F., Brigham, D., Belli, B., Karaman, M.W., Pratz, K.W., Pallares, G., Chao, Q., et al. (2009). AC220 is a uniquely potent and selective inhibitor of FLT3 for the treatment of acute myeloid leukemia (AML). *Blood* *114*, 2984–2992.
- Zhu, H.H., Ji, K., Alderson, N., He, Z., Li, S., Liu, W., Zhang, D.E., Li, L., and Feng, G.S. (2011). Kit-Shp2-Kit signaling acts to maintain a functional hematopoietic stem and progenitor cell pool. *Blood* *117*, 5350–5361.